Article

J. Biol. Regul. Homeost. Agents. 2024; 38(5): 3685–3698
https://doi.org/10.23812/j.biol.regul.homeost.agents.20243805.291

The Repression of the *Candida albicans* Growth and Pseudomycelium Formation by Thiomonoterpenoid

Svetlana A. Lisovskaya[1,2,3,*], Alexander A. Ksenofontov[4], Pavel S. Bocharov[4], Elena V. Antina[4], Galina B. Guseva[4], Mikhail B. Berezin[4], Ilmir R. Gilfanov[2,5], Roman S. Pavelyev[2], Matvey O. Sabantsev[2], Olga V. Ostolopovskaya[1,2], Elena Y. Trizna[2], Svetlana V. Pestova[6], Evgeniy S. Izmest'ev[6], Svetlana A. Rubtsova[6], Andrei G. Izmailov[1], Albert A. Rizvanov[2,7], Liliya E. Nikitina[1,2,8], Airat R. Kayumov[2,7]

[1]Faculty of Medicine and Biology, Kazan State Medical University, 420012 Kazan, Russia
[2]Institute of Fundamental Medicine and Biology, Kazan Federal University, 420008 Kazan, Russia
[3]Kazan Scientific Research Institute of Epidemiology and Microbiology, 420015 Kazan, Russia
[4]G.A. Krestov Institute of Solution Chemistry of Russian Academy of Sciences, 153045 Ivanovo, Russia
[5]Institute of Petroleum, Chemistry and Nanotechnologies, Kazan National Research Technological University, 420015 Kazan, Russia
[6]Institute of Chemistry, Federal Research Center "Komi Scientific Centre", Ural Branch, Russian Academy of Sciences, 167000 Syktyvkar, Russia
[7]Division of Medical and Biological Sciences, Tatarstan Academy of Sciences, 420111 Kazan, Russia
[8]Division of Chemistry and Chemical Technologies, Tatarstan Academy of Sciences, 420111 Kazan, Russia
*Correspondence: s_lisovskaya@mail.ru (Svetlana A. Lisovskaya)
Published: 1 May 2024

Background: In the last decade, the wide spread of the multidrug resistant yeast *C. albicans* has challenged the development of new approaches to treatment. Among various options, the use of natural and synthetic terpenes as antifungals or enhancers of conventional drugs has been offered in many works. Here we show the effect of the recently synthesized compound isobornane sulfide named KS1 on *C. albicans* and discuss its potential mechanism of action.

Methods: To characterize the impact of the compound on the yeast minimum inhibitory concentration (MIC) determination on clinical isolates, quantitative PCR with reverse transcriptase (qRT-PCR) of efflux genes expression, cytotoxicity determination on eukaryotic cells, bright-field and fluorescent microscopy with KS1 conjugate with BODIPY fluorophore have been used. The *in silico* prediction of KS1 properties has been performed using the ADMET server, and molecular docking was used for the modeling of KS1 interaction with putative targets.

Results: While exhibiting moderate antifungal activity as compared to fluconazole and terbinafine, KS1 has a synergy with both antifungals on resistant clinical isolates while not stimulating the expression of the *CDR1* and *MDR1* efflux genes. Moreover, KS1 represses hypha formation by *C. albicans*, reducing the number of germ tubes more than twice compared to the control. It readily penetrates the cell, as shown by confocal microscopy using the created KS1-BODIPY fluorophore conjugate, apparently thereby facilitating the penetration of antifungals into the cell. As judged by the ADMET server, KS1 falls into the category of drug-like compounds and neither inhibits the isoforms of cytochrome P450 nor manifests mutagenicity or carcinogenicity that fits with *in vitro* data. The molecular docking showed that KS1 has a high affinity for the transcription activator transcription activator (Tec1) protein of *C. albicans*, responsible for invasion and hypha formation, which fits with the *in vitro* data.

Conclusions: These findings suggest KS1 as promising both a solely antifungal and an enhancer of conventional antimycotics blocking fungal virulence.

Keywords: *Candida albicans*; synergistic effect; monoterpenoids; molecular docking

Introduction

Over the past few decades, the frequency of factors reducing the overall resistance and immune response of the human body has continuously elevated, thereby increasing the risk of diseases caused by opportunistic bacterial and fungal pathogens. Candidiasis caused by fungal species of the *Candida* genus, especially *Candida albicans*, is found in the mouth cavities, vaginas, and bowels of 20–70% of the examined persons. Candidiasis represents up to 37% of all infectious human diseases and up to 86% of all fungal human diseases [1–4].

To date, the efficiency of candidiasis treatment has decreased [5–7]. While conventional antimycotics were manifested to exhibit fungicidal activity, there is an alarming trend in the increasing resistance of *Candida* to azoles and

Copyright: © 2024 The Author(s). Published by Biolife Sas. This is an open access article under the CC BY 4.0 license.
Note: *J. Biol. Regul. Homeost. Agents.* stays neutral with regard to jurisdictional claims in published maps and institutional affiliations.

Journal of
BIOLOGICAL REGULATORS
and Homeostatic Agents

synthetic antifungals, such as fluconazole, that are widely used clinically [8]. This is explained both by the unreasonably wide use of azoles and by the reduction of responsiveness to fluconazole [9]. Therefore, various approaches affecting the fungus virulence factors instead of killing the pathogen are proposed today as a new, promising antifungal strategy to ensure the natural elimination of infectious agents from the macroorganism without the development of resistance [10]. Among such approaches, the use of essential oils or crude phytoextracts is widely offered [11–13], where various terpenes and terpenoids are the active components. These compounds have been shown to be both enhancers of conventional drugs and solely antifungals, although with moderate activity [14–21]. Being of small size, these compounds and their conjugates with other pharmacophores could penetrate cells and affect them. Thus, the activity of fluconazole has been reported to be significantly increased by myrtenol [19] and a conjugate of borneol with 2(5*H*)furanone [18], suggesting these molecules as promising adjuvants.

C. albicans has various virulence factors that ensure the ingress of infection into various loci of the macroorganism, like the pseudohyphae formation, the expression of adhesins and invasins, synthesis of hydrolytic enzymes, the hypha-associated proteins Hwp1, Hyr1, agglutinin-like sequence-3 (Als3) and Ece1, as well as the biofilm formation [1,22]. Revealing the pathogenicity mechanisms of *C. albicans* opens the door for the development of new techniques for antifungal treatment. Genetic studies allowed identifying genes that code secreted proteolytic enzymes, i.e., the *C. albicans* secreted aspartic proteases (Saps), which contribute to performing specialized functions during the infection process. Thus, the aspartic proteases Sap4, Sap5, and Sap6 ensure *C. albicans* adhesion and penetration through mucous membranes into the deep tissues [1,23].

In this paper, we show the effect of the recently synthesized compound isobornane sulfide, named **KS1**, on *C. albicans* and discuss its potential mechanism of action. While exhibiting moderate fungicidal activity, **KS1** enhances *in vitro* the activity of conventional antifungals and antiseptics as well as represses hyphae formation by the yeast.

Materials and Methods

Synthesis

The isobornane sulfide named **KS1** (Fig. 1) was synthesized according to [24]. Briefly, to a solution of isobornanethiol (221 mg) in ethanol (3 mL, #130523, ROSBIO, St. Petersburg, Russian Federation), Cs_2CO_3 (424 mg, #10216654, Alfa Aesar, Lancashire, UK), and tetrabutylammonium iodide (480 mg, #10163887, Alfa Aesar, Lancashire, UK) were added under an argon atmosphere. After stirring for 5 min, 2-bromoethanol (71 µL, #124832, Grankhim, Chelyabinsk, Russian Federation) was added dropwise, and the mixture was refluxed for 24 h. The obtained solution was filtered, concentrated and purified by silica gel column chromatography using petroleum ether–EtOAc (1:1) as an eluent. All reagents were analytical grade. The isobornane sulfide **KS1** was obtained as a liquid in 90% yield, $[\alpha]_D^{20} = +248°$ (*c* 0.3, $CHCl_3$). Synthesis, physicochemical properties, and spectral data of BODIPY **2** and its fusion with **KS1 3** were described previously [25–27].

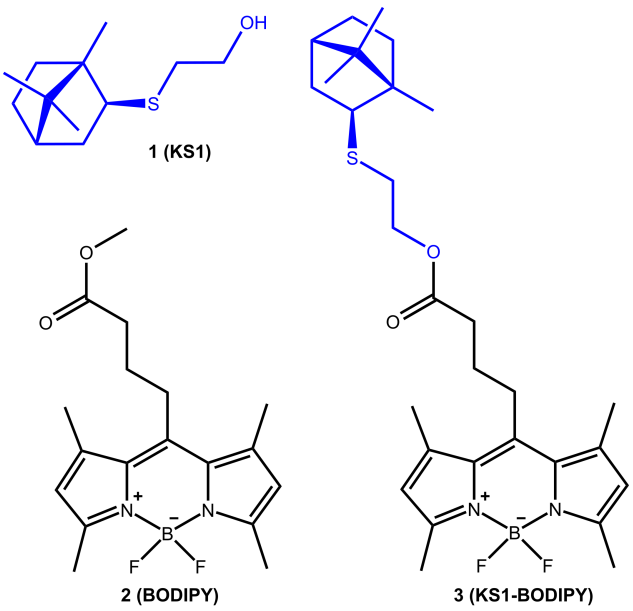

Fig. 1. Structures of the compounds used in the study. KS1 (**1**), BODIPY (**2**) and its fusion with **KS1** (**3**).

Molecular Docking

ADMET and Drug-likeness Properties

To evaluate ADMET and drug-likeness properties of compounds **1** and **2**, the online service ADMETlab 2.0 (https://admetmesh.scbdd.com/) [28] was used. Antifungal drugs, fluconazole and terbinafine, which are applied in the treatment and prevention of candidiasis and some other mycoses were used as reference compounds.

Molecular Docking

Ligand-receptor systems modeling was performed using Autodock 4.2 software (https://autodock.scripps.edu/) [29]. The initial ligand structures (**KS1**, fluconazole, and terbinafine) were optimized using the CAMB3LYP functional [30] and auq-cc-pVTZ basis [31]. The structures of putative target proteins Sap1-3, 5 and Agglutinin-like sequence-3 (Als-3) were obtained from the protein database https://www.rcsb.org/ (1EAG, 2H6S, 2QZW, 2QZX, 4LE8, respectively). The structures of phospholipase b1 (Plb1) (ProteinBankID:AAC72296.1) and Transcription activator Tec1 (ProteinBankID: KAF6072269.1)

were modeled by the Swiss-model [20,21]. For each system, a grid of force fields (grid) was built, in which further calculations took place. For 1eag we chose grid 80 Å × 90 Å × 126 Å with a 0.650 Å step, 2h6s 126 Å × 126 Å × 126 Å with a 0.500 Å step, 2qzw 126 Å × 126 Å × 126 Å with a 0.670 Å step, 2qzx 81 Å × 81 Å × 90 Å with a 0.670 Å step, Als3 100 Å × 70 Å × 126 Å with a 0.650 Å step, Plb1 126 Å × 100 Å × 100 Å with a 0.820 Å step, and Tec1 100 Å × 100 Å × 126 Å with a 0.820 Å step. Next, molecular docking was carried out, in which the structures of the ligands were accepted to be flexible and the structures of the receptors were accepted to be rigid, and the calculation was carried out using the Lamarck genetic algorithm [32] with 50 separate runs ending after 25 million energy evaluations per each calculation. The ligand-receptor complexes were sorted into groups according to RMSE. For each ligand-receptor complex, the lowest energy conformation was considered the most stable.

Biological Assays

Strains and Growth Conditions

The study was carried out on clinical yeast isolates (14 isolates) isolated from the pharyngeal mucosa and obtained from the collection of the Kazan Institute of Microbiology and Epidemiology (Kazan, Russia). To obtain a working suspension, yeasts were grown on Sabouraud agar for 48 h and washed with a sterile isotonic sodium chloride solution.

Antimycotic Activity

Determination of the minimum inhibitory concentrations (MICs) of compounds *in vitro* was performed according to the CLSI M27-A3 protocol by the microdilution assay in Roswell Park Memorial Institute (RPMI) 1640 medium with 0.2% glucose without bicarbonate (CC330-50/12.3.2022, PanEco, Moscow, Russia) [33,34]. A suspension containing 1–5 × 10^5 yeast cells was prepared in a sterile isotonic sodium chloride solution by washing the cells from the agar plates. The tubes were incubated for two days at 37 °C with visual control of the growth. The minimum inhibitory concentration (MIC) was considered as the minimum concentration of the compound providing complete suppression of the visible growth of test strains. As a reference, the conventional antimycotics fluconazole and terbinafine were used.

Synergy Testing between **KS1** and Antifungals

To assess a synergy between **KS1** and antifungals (fluconazole and terbinafine lots 7D013030, SLBR5903V, Sigma-Aldrich, St. Louis, MO, USA), a checkerboard assay was performed using standard procedure [35]. Yeast was grown in a way similar to MIC testing in 96-well plates using RPMI 1640 medium with 0.2% glucose without bicarbonate (CC330-50/12.3.2022, PanEco, Moscow, Russia). After a series of two-fold dilutions, the concentrations of **KS1** in wells were 1.5–192 µg/mL. The concentrations of fluconazole were 0.375–96 µg/mL; the concentrations of terbinafine were 0.375–24 µg/mL. The plates were incubated for 48 h at 37 °C under static conditions. Each test was performed three times and contained the growth control of bacteria without antifulgals. The fractional inhibitory concentration index (FICI) for combinations of **KS1** with antifungals was calculated as follows:

$$\text{FICI} = \frac{\text{MIC [A] in combination}}{\text{MIC [A]}} + \frac{\text{MIC[B] in combination}}{\text{MIC [B]}} \quad (1)$$

Interpretation of the FICI values was carried out according to [35]: FICI $\leq$0.5 indicated as synergy, 0.5 < FICI $\leq$ 4 is an additive effect, and FICI >4 indicated antagonism.

Table 1. The oligonucleotides used for the qRT-PCR.

Name	Sequence
q*GAPDH* for	5′ GTCTCCTCTGACTTCAACAGCG 3′
q*GAPDH* rev	5′ ACCACCCTGTTGCTGTAGCCAA 3′
q*CDR1* for	5′ GTACTATCCATCAACCATCAGCACTT 3′
q*CDR1* rev	5′ GCCGTTCTTCCACCTTTTTGTA 3′
q*MDR1* for	5′ TCAGTCCGATGTCAGAAAATGC 3′
q*MDR1* rev	5′ GCAGTGGGAATTTGTAGTATGACAA 3′

GAPDH, glyceraldehyde-3-phosphate dehydrogenase; qRT-PCR, quantitative PCR with reverse transcriptase.

Evaluation of Resistance Development in Serial Passage Experiments

The *in vitro* resistance development of fungi was studied in a serial passage protocol as described in [36], with modifications described by Garipov *et al*. [34]. Briefly, yeasts were seeded in RPMI medium with 2-fold serial dilutions of the test compounds and grown similarly as in the MIC-determining assay. The cells from the tubes with the highest concentration of compounds allowing fungal growth were used as inoculum for the next passage. The procedure was repeated seven times, and MICs were recorded in each passage. Cells growing at the highest concentration of compounds after the 7th passage were harvested and subjected to quantitative real-time PCR analysis of the transcription level of the efflux system genes *MDR1* and *CDR1*.

RNA Isolation and Real-time One-step qRT-PCR

To determine the transcription level of the efflux system genes *MDR1* and *CDR1* was evaluated using quantitative real-time PCR (Extra Mix for Reverse Transcription with SYBR Blue, Cat. RM03, BioLabMix, Novosibirsk, Russia) on a PCR amplifier “BioRad CFX96” (Bio-Rad, Foster, CA, USA). The oligonucleotides used for the quantitative PCR with reverse transcriptase (qRT-PCR) are shown in Table 1 [37–39]. A total RNA was extracted from *C. albicans* cells grown on the seventh cycle at the highest concentration of either fluconazole or **KS1** in *in vitro* resistance development assay. The RT-PCR program included

Journal of
BIOLOGICAL REGULATORS
and Homeostatic Agents

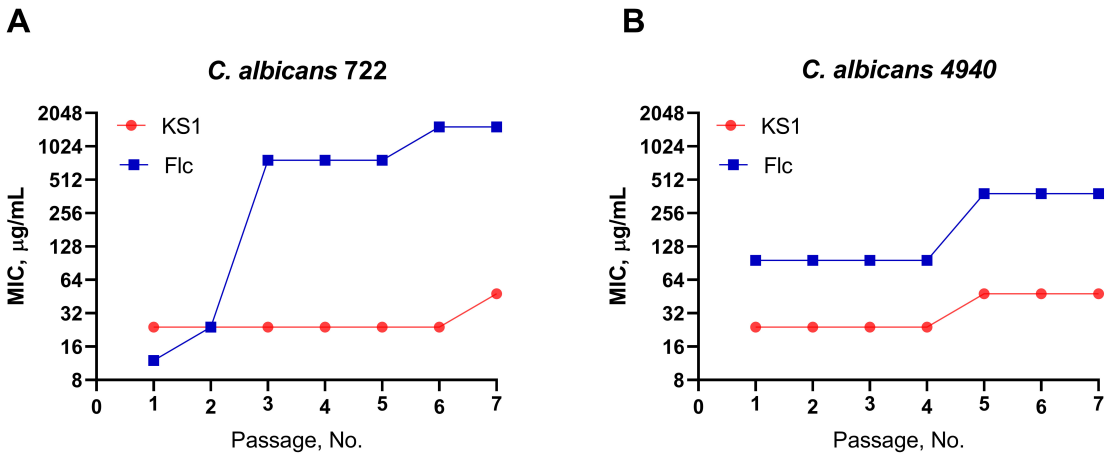

Fig. 2. The development of resistance to KS1 and fluconazole in 7 passages in liquid medium. The (A) sensitive (*C. albicans* 722) and (B) resistant (*C. albicans* 4940) isolates were grown for 24 h in Roswell Park Memorial Institute (RPMI) medium in the presence of different concentrations of compounds. Cells grown at highest concentration of compounds were used as inoculum for the next seeding cycle. The data are presented as medians from four independent experiments. MIC, minimum inhibitory concentration.

reverse transcription at 45 °C for 30 min, followed by 37 cycles of melting – primer annealing – elongation. Primer annealing temperatures were calculated using the Tm Calculator service (https://tmcalculator.neb.com). The cycling thresholds (Ct) of *CDR1* and *MDR1* genes were normalized using the glyceraldehyde-3-phosphate dehydrogenase (*GAPDH*) gene expression level as a reference; next, the relative transcription level of the *CDR1* and *MDR1* genes was quantified using the $2^{-\Delta\Delta Ct}$ method and are shown as fold increase of the *CDR1* and *MDR1* transcriptions after exposition to antifungals compared to untreated cells.

Effect of Test Substances on the Formation of Candida albicans Germ Tubes (Filament Initiation)

The impact of **KS1** and conventional antifungals on the initiation of embryonic tubes formation by *C. albicans* was investigated by incubating the blastospora of the sensitive (*C. albicans* 722) and resistant (*C. albicans* 4940) isolates in Sabouraud broth supplemented with 10% hemoglobin powder (lot 3275839, HiMedia Laboratories, Modautal, Germany) at a temperature of 37 °C during six hours. A comparative percentage of the inhibition of germinal tube formation was determined by microscopy, followed by a semi-automatic count of tubes and spheric cells by original approach [40,41]. The study was performed with sublethal quantities of compounds (corresponding to their respective 0.5 MIC, 0.25 MIC, and 0.125 MIC) [42].

Assessment of Penetration of **KS1** into the Microscopic Fungal Cell and Biofilm

Yeast cells were stained with BODIPY (2 mg/mL) for 20 min. The cell wall of yeasts has been stained with Calcofluor White (CFW), which interacts with chitin and cellulose. The microscopic analysis has been performed on the Carl Zeiss AxioScope.A1 Microscope (Carl Zeiss AG, Jena, Germany), equipped with an oil immersion objective with 63× magnification. BODIPY and CFW were visualized in green (497–524 nm) and blue (358–463 nm) channels, respectively. Data were analyzed with ZEN 9.0 software (Carl Zeiss AG, Jena, Germany). The penetration of **KS1** into the yeast biofilms was assessed with Confocal laser scanning microscopy. Biofilms were grown for 48 h in RPMI 1640 medium in a 8-wells cell imaging chambered coverslip (lot 211202/6, Ibidi, Gräfelfing, Germany). Then biofilms were stained with Calcofluor White (25 μM) and BODIPY **2** (2 mg/mL) or **KS1**-BODIPY **3** (2 mg/mL) for 20 min and analyzed by an Olympus IX83 inverted microscope (Olympus Europa, Hamburg, Germany) supplemented with a STEDYCON ultrawide extension platform (Abberior, Göttingen, SY194701, Germany).

Assessment of Mutagenicity and Cytotoxicity of **KS1**

The mutagenicity of **KS1** was evaluated in the Ames test on *S. typhimurium* TA98, TA100, and TA102 strains as described by McCann and Ames [43], with the spot-test modification to avoid false-negative results because of the antibacterial activity of the compounds. The compound was considered mutagenic if the increased number of revertant colonies was observed close to the filter paper with the compound.

The cytotoxicity of **KS1** was determined by using the microtetrazolium test (3-(4,5-dimethylthiazol-2-yl)-2,5-diphenyltetrazolium bromide (MTT) (lot 010543722, PanEco, Moscow, Russia) on bovine embryonic lung epithelial cells (LEK) (from the Russian Collection of Cell Cultures of Vertebrates (CCCV)) and primary human skin fibroblasts (HSF) isolated previously [44]. For all cell cultures, the absence of contamination with mycoplasma has been confirmed by PCR. The cells were cultured in DMEM – Dulbecco's Modified Eagle's Medium (lot C425P74,

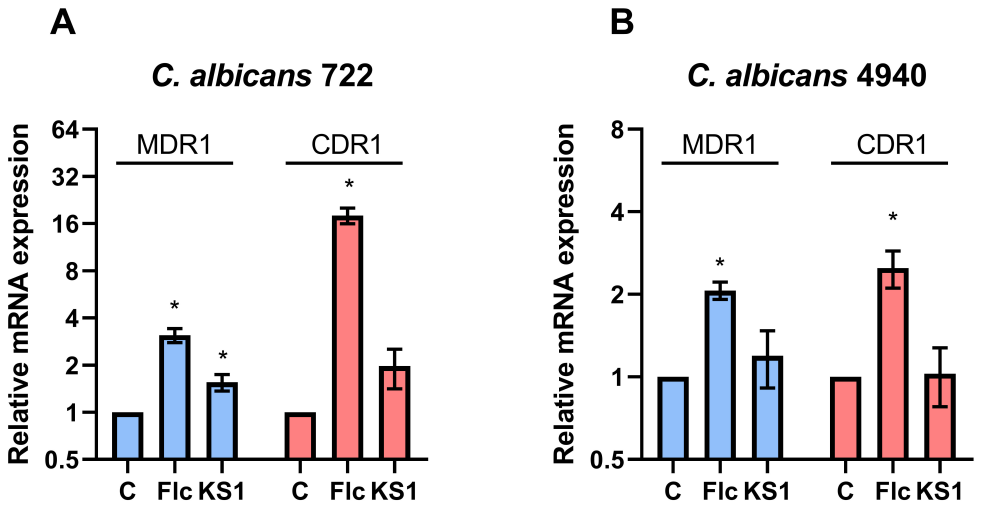

Fig. 3. Relative expression levels of efflux system genes *CDR1* and *MDR1* in *C. albicans* on 7th passage with sub-lethal concentrations of fluconazole (Flc) and KS1. The (A) sensitive (*C. albicans* 722) and (B) resistant (*C. albicans* 4940) isolates were subsequently seeded in RPMI medium in the presence of sub-MIC of compounds, and cells harvested after 7th passage (see Fig. 2) were harvested, and the expression of *MDR1* and *CDR1* was assessed by quantitative RT-PCR. Data are presented as averages with SD from four biological repeats. The data are normalized for the control group (untreated cells). The *GAPDH* gene was used as a reference. Asterisks denote a significant difference with untreated cells (Control, C) in a multiple *t*-test with Holm-Sidak correction ($p < 0.05$).

PanEco, Moscow, Russia), supplemented with 10% FBS (lot S00MY1000B, Biosera, Kansas, MO, USA), 2 mM L-glutamine, 100 µg/mL penicillin, and 100 µg/mL streptomycin. Cells were seeded in 96-well plates with a density of 3000 cells per well and cultured at 37 °C with 5% CO_2. After 24 h, compound was added in concentrations ranging from 1 to 1024 µg/mL, and cultivation was continued for the next 24 h. The residual metabolic activity was assessed by the MTT-assay and the concentration of compound leading to a two-fold reduction of metabolic activity (CC_{50} value) was calculated.

Statistical Analysis

All experiments were carried out three independent replicates or as indicated. The results were analyzed for statistical significance with either multiple *t*-test (when comparing means) or Kruskal–Wallis test (when comparing medians) with Holm-Sidak correction by GraphPad Prism 6.0 software (GraphPad Software Inc., San Diego, CA, USA). Differences were considered as significant at $p < 0.05$. The CC_{50} values were calculated by using GraphPad Prism 6.0 software with four-parameters model and agonist concentrations in log-scale.

Results

Antifungal Activity and Synergistic Effect with Other Antifungals

The antimycotic activity was studied on a series of *Candida albicans* clinical isolates, fluconazole and terbinafine served as reference drugs. **KS1** exhibited antifungal properties, with MIC values being in the range of 12–48 µg/mL (See Table 2). Of note, the activity of **KS1** against clinical strains was comparable with fluconazole or exceeded it 2–4 times. In turn, the MICs of terbinafine were typically four times lower as compared to **KS1**.

Table 2. Antifungal activity of compounds. MICs, µg/mL.

Strains	KS1	Fluconazole	Terbinafine
C. albicans C-2210-19	24	96	6
C. albicans C-6175-19	48	96	6
C. albicans C-6198-19	12	12	3
C. albicans C-6248-19	12	12	3
C. albicans C-6249-19	24	24	6
C. albicans C-6296-19	24	48	12
C. albicans C-6284-19	48	96	6
C. albicans C-6337-19	24	24	12
C. albicans C-6401-19	48	96	12
C. albicans 761	24	12	12
C. albicans 4940	48	96	12
C. albicans 701	48	96	12
C. albicans 762	48	48	6
C. albicans 722	24	12	6

MICs, minimum inhibitory concentrations.

Since for various terpenes and their derivatives a synergy with antifungals has been reported previously [18,19], the ability of **KS1** to reduce the MIC of antifungals (fluconazole and terbinafine) has been tested on five clinical isolates of *C. albicans*. The values of the FICI were determined as described in the materials and methods, and the median value from several wells was calculated. Table 3 shows that **KS1** significantly decreases the MIC of

Journal of
BIOLOGICAL REGULATORS
and Homeostatic Agents

Table 3. MIC, FIC and FICI values of KS1, Fluconazole and Terbinafine on *C. albicans* isolates, µg/mL.

Isolates	MIC			FIC				FICI	
	KS1	Fluc	Terb	**KS1**	Fluc	**KS1**	Terb	Fluc+**KS1**	Terb+**KS1**
C. albicans 761	24	12	12	6	6	6	3	0.75	0.50
C. albicans 4940	48	96	12	12	1.5	12	1.5	0.26	0.375
C. albicans 701	48	96	12	12	2	12	1.5	0.27	0.375
C. albicans 762	48	48	6	12	12	12	1.5	0.50	0.50
C. albicans 722	24	12	6	6	6	6	3	0.75	0.75

FIC, fractional inhibitory concentration; FICI, fractional inhibitory concentration index; Fluc, fluconazole; Terb, terbinafine.

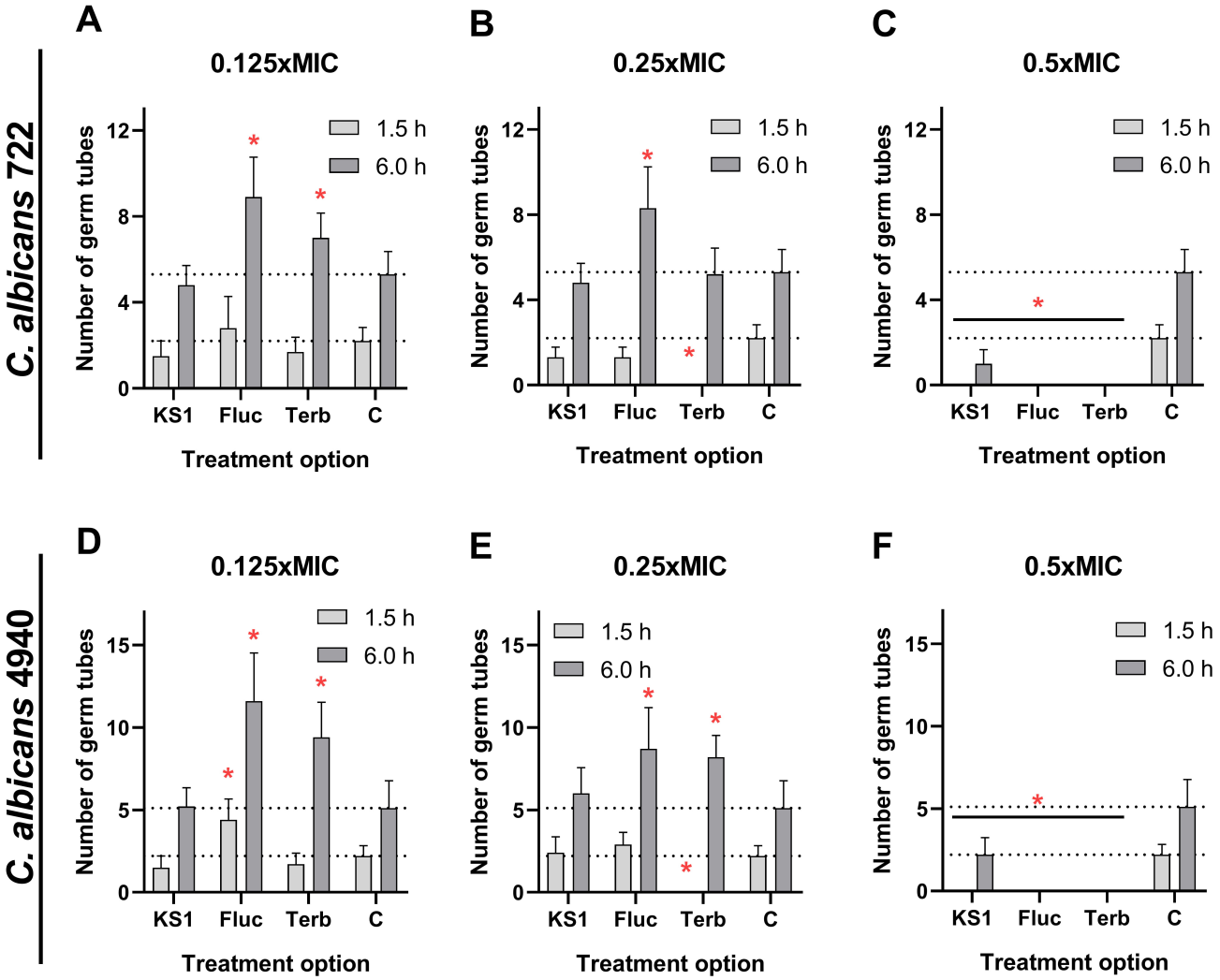

Fig. 4. The pseudomycelium formation by *C. albicans* fluconazole-sensitive (*C. albicans* 722, A, B, C) and -resistant (*C. albicans* 4940 D, E, F) isolates in the presence of sub-lethal concentrations of fluconazole (Fluc), terbinafine (Terb) and KS1. The blastospora of *C. albicans* isolates were grown in Sabouraud broth supplemented with 10% hemoglobin powder at 37 °C for six hours and analyzed by microscopy. Data are presented as averages with SD from 10 fields of view. Asterisks (*) denote a significant difference with untreated cells at respective time point (Control, C) in a multiple *t*-test with Holm-Sidak correction ($p < 0.05$ vs Control).

fluconazole against strains with low sensitivity to this antifungal, demonstrating marked synergism with the FICI of 0.26–0.27. Additionally, marked synergy has been observed also for terbinafine, with FICI values of 0.375–0.5. Interestingly, only an additive effect could be observed for strains sensitive to antifungals. This fact allows speculation that **KS1** apparently facilitates the penetration of drugs into the yeast cell.

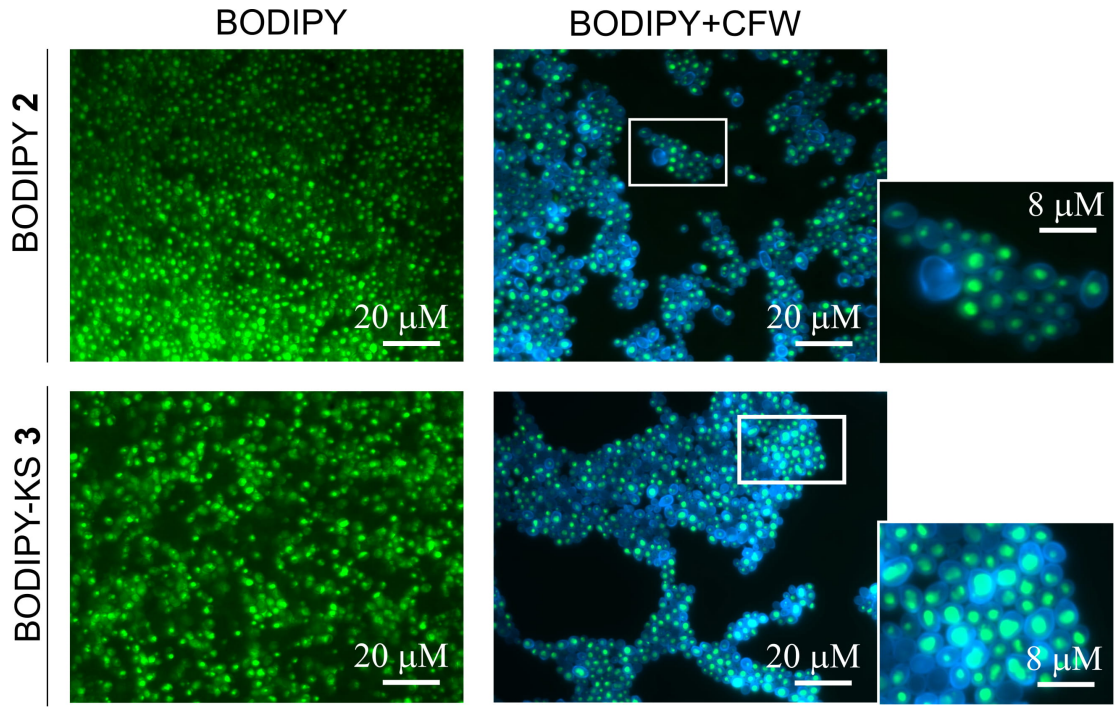

Fig. 5. Penetration of BODIPY 2 and KS1-BODIPY conjugate 3 into *C. albicans* cells. *C. albicans* 722 cells were treated for 20 min with either pure BODIPY 2 or and KS1-BODIPY conjugate 3. Then cells were stained with CalcoFluor white and analyzed by the Carl Zeiss AxioScope.A1 with a magnification of 10 × 40. Scale bar = 8 μm, 20 μm.

*Evaluation of in Vitro Resistance Formation to **KS1** and Efflux Genes Activation*

Spontaneous resistance development was studied as described in materials and methods on two isolates, which were sensitive (*C. albicans* 722) and resistant (*C. albicans* 4940) to fluconazole. For the sensitive strain, the MIC of fluconazole increased significantly (up to 8-fold) on the 3rd passage day of cultivation (Fig. 2A), while no such effect has been observed for the resistant strain (Fig. 2B). In turn, the sensitivity of both *C. albicans* strains to **KS1** did not change significantly (Fig. 2).

The expression of drug efflux pumps withdrawing various toxins and drugs from the cell, is one of the mechanisms of elevated tolerance of *C. albicans* to antifungals resistance [37]. The *CDR1* and *MDR1* pumps are believed to be the most frequently observed effluxes responsible for resistance to azoles and their expression has been reported to be induced in presence of antifungals [37–39]. To evaluate the ability of **KS1** to induce the expression of these efflux pumps thus providing the development of multidrug resistance phenotype, the expression of efflux system genes *MDR1* and *CDR1* in cells of both isolates was investigated by qRT-PCR analysis of mRNA after 7th passage. When growing in presence of fluconazole, the expression level of both genes increased significantly in both isolates, up to 20-fold for *CDR1* in *C. albicans* 722, which fits with resistance development (compare Fig. 2A with Fig. 3A, and Fig. 2B with Fig. 3B). In marked contrast, the presence of **KS1** did not lead to induction of the mentioned genes since the coefficients of relative expression of *MDR1* and *CDR1* were less than 2 (Fig. 3).

Repression of the Pseudomycelium Formation

The effect of **KS1** and conventional antifungals on germ-tubes and pseudomycelium formation by *C. albicans* was evaluated by calculation of the number of germinating tubes after 1.5 and 6 h of growth in the presence of **KS1** and conventional antifungals at the concentrations corresponding to their respective 0.5×, 0.25×, and 0.125× MICs (see Table 2 for values). Ten fields of view have been analyzed and averaged. While both antifungals repressed the pseudomycellium formation at 0.5× MIC, up to at least two-fold increase in the germ tube number of both strains has been observed at 0.125× MICs of luconazole as compared to untreated cells (Fig. 4). Terbinafine at 0.125× MICs also led to an increase in germ tube number by factor 1.5–2, suggesting increased invasion ability of yeast in response to treatment. While in the presence of 0.5× MIC of **KS1** a few germ tubes could be observed after 6 h, the number of the latter was 2–4 fold less as compared to untreated cells, suggesting that **KS1** represses the ability of *C. albicans* for invasion.

Journal of
BIOLOGICAL REGULATORS
and Homeostatic Agents

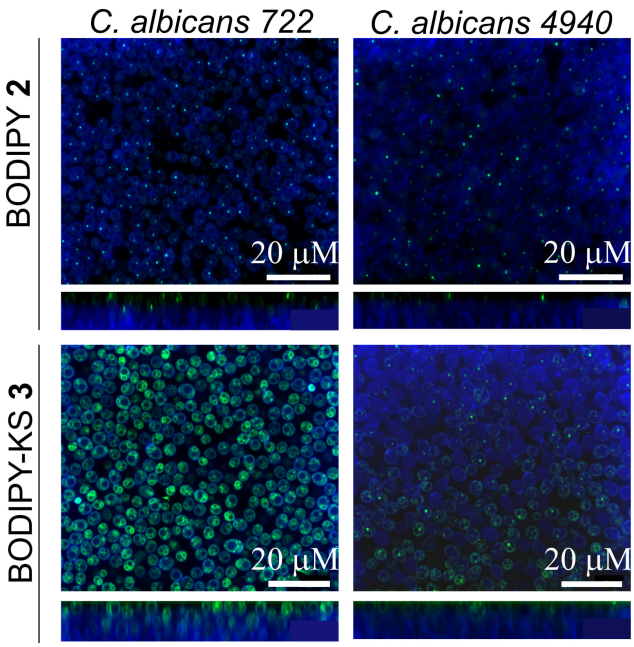

Fig. 6. Penetration of BODIPY 2 and KS1-BODIPY conjugate 3 into *C. albicans* biofilm embedded cells. Microbial 48 h-old biofilms were treated for 20 min with either pure BODIPY 2 or and **KS1**-BODIPY conjugate 3. Then cells were stained with CalcoFluor white and analyzed by Olympus IX83 inverted microscope supplemented with a STEDYCON ultrawide extension platform with a magnification of 20 × 100. Scale bar = 20 μm.

*Assessment of **KS1** Penetration into the Fungal Cells and Biofilm*

Further, the ability of **KS1** to penetrate into the fungal cell has been assessed. For that, **KS1** was fused with BODIPY **2** to obtain the **KS1**-BODIPY conjugate **3** (see Fig. 1 for the structures). The *C. albicans* cells were stained with either **2** or **3** (in concentrations of 2 μg/mL) and Calcofluor White (CFW) for 20 min and then analyzed with microscopy (Fig. 5). BODIPY **2** stained the cytoplasmic cell content without any pronounced edge of cytoplasmic membranes. Penetration of **3** into *C. albicans* cells was observed immediately after staining with the pronounced cell edge fluorescence upon 20 minutes of treatment. Interestingly, the fluorescence intensity was basically observed on the membrane of organelles, while staining of the cell membrane was not detected. Of note, BODIPY **2** penetrated poorly the "old" cells of the *C. albicans*, which have many bud scars acquired during multiple reproductions (budding) of fungi, while conjugate **3** was able to penetrate all cells (Fig. 5).

Then, the penetration of **KS1** into biofilms of *C. albicans* formed by either sensitive (isolate 722) or resistant (isolate 4940) to fluconazole has been evaluated with confocal laser scanning microscopy. The 48-h old biofilms were stained similarly to planktonic cells as described above and analyzed with CLSM (Fig. 6). As can be seen from the figure (Fig. 6), pure BODIPY **2** dissociates poorly into the biofilm matrix of both isolates. By contrast, **KS1**-BODIPY conjugate 3 quickly penetrates into cells of sensitive strain and more slowly into cells of resistant strain.

Cytotoxicity and Mutagenicity

The cytotoxicity of **KS1** was evaluated by using bovine embryonic lung epithelial cells (LEK) and primary human skin fibroblasts (HSF). The CC_{50} of **KS1** was found to be 175 ± 1 μg/mL for LEK and 101 ± 4 μg/mL for HSF (Fig. 7), thus being suitable for the topical application. To evaluate the genotoxicity of **KS1**, the Ames test was carried out using *S. typhimurium* TA98, TA100, and TA102 strains in a spot-test. In all strains studied, no increase in the number of revertants was detected close to the disk, suggesting no mutagenic potential of **KS1**.

Molecular Docking

The data above demonstrated that **KS1** represses the pseudomycelium formation by *C. albicans*, suggesting that the proteins responsible for invasion and important regulators of the *C. albicans* virulence factors, including Saps, agglutinin-like sequence-3 (Als3), phospholipase b1 (Plb1), and transcription activator (Tec1), which regulate certain stages of the infectious process [45–47] and previously identified as putative targets for terpenes [20,21], could be potential targets for **KS1**. We carried out molecular docking for **KS1** with these proteins, to determine the binding sites and evaluate the protein-ligand interaction energy. Fluconazole and terbinafine were used as reference ligands.

Analysis of the free binding energies (ΔG_{bind}) of **KS1** and reference drugs with Saps, Als3, Plb1, and Tec1 confirmed their high affinity for these protein targets (Fig. 8). The affinity of compounds to active sites of virulence-associated proteins increases in the sequences Sap1 – Sap2 – Sap5 – Plb1 – Sap3 – Als-3 – Tec1 for **KS1**, Sap1 – Plb1 – Sap5 – Tec1 – Sap2 – Als3 – Sap3 for fluconazole, and Tec 1 – Als3 – Plb1 – Sap5 – Sap1 – Sap3 – Sap2 for terbinafine. Although the differences in free energies are small, it can be noted that **KS1** has the highest affinity to Tec1, Als-3 and Sap3. Fluconazole and terbinafine have higher affinity for Sap3, Sap2, Als3 and Sap2, Sap3, Sap1, respectively.

Next, we consider in more detail the binding sites structure in the most stable ligand-protein supramolecular complexes. The amino acid composition of the binding sites is shown in Fig. 9, **Supplementary Fig. 1**. In the Tec1–**KS1** complex, the ligand is localized in the protein pocket near the L1 loop, which is formed by the amino acid residues ILE198, PRO199, ASN204, LYS205, ILE206, LYS207, CYS213, GLY214, ARG215, and LEU218. In the Als3–**KS1** complex, the thiotherpenoid is localized in the pocket of the N-terminal domain of Als3 [48]. The amino acid composition of this pocket is characterized by LYS59, PHE60, THR62, SER63, GLN64, THR65, PHE81,

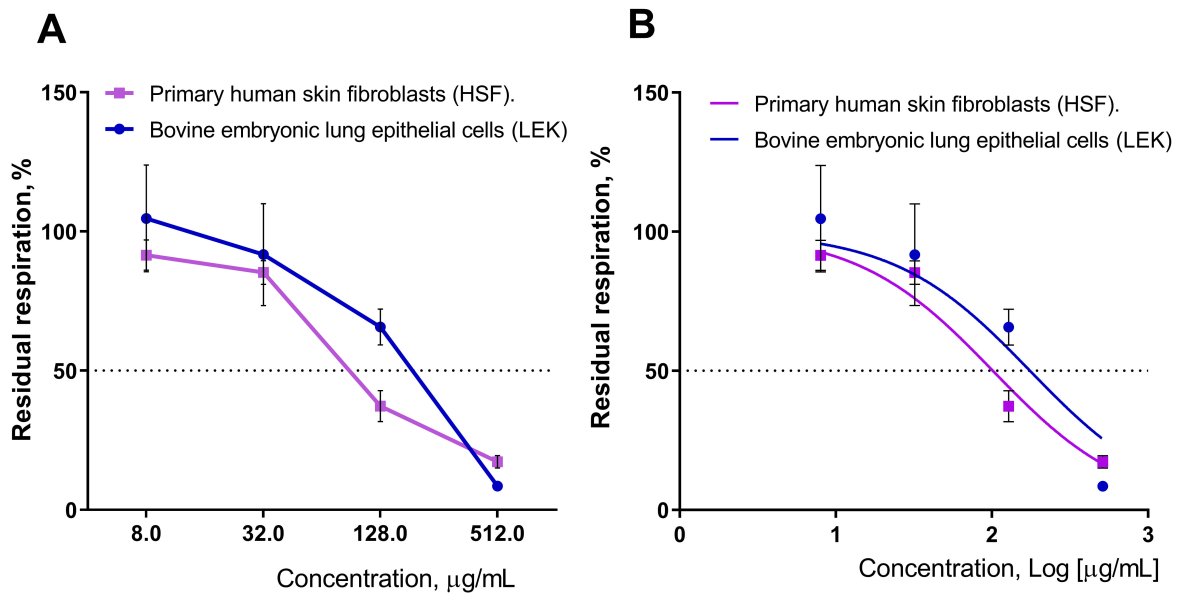

Fig. 7. Cytotoxicity of KS1 against eukaryotic cells. The bovine embryonic lung epithelial cells (LEK) and primary human skin fibroblasts (HSF) cells were cultured in DMEM in presence of **KS1** for 24 h and the residual metabolic activity was assessed by the 3-(4,5-dimethylthiazol-2-yl)-2,5-diphenyltetrazolium bromide (MTT)-assay (A) and a two-fold reduction of metabolic activity (CC_{50} value) value was calculated (B).

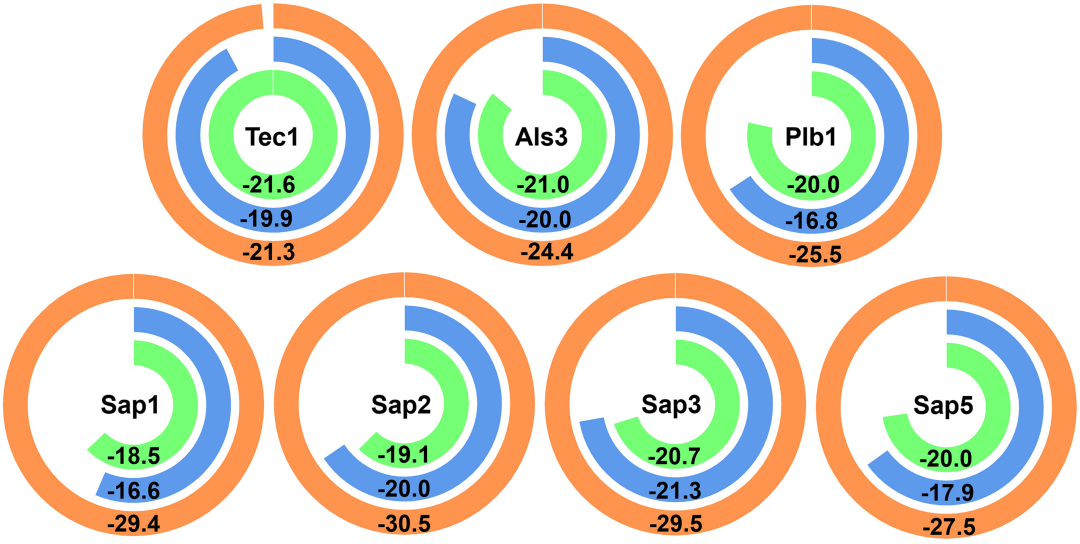

Fig. 8. The donut plots of binding free energy (kJ/mol) of compounds to target proteins. KS1 (green), fluconazole (blue), and terbinafine (orange). Saps, secreted aspartic proteases; Tec1, transcription activator; Als3, agglutinin-like sequence-3; Plb1, phospholipase b1.

GLN82, ALA83, GLU85, PHE87, PRO174, and SER175. In Sap3, **KS1** is located in the pocket near the C-ent loops. The amino acid composition of binding sites includes VAL203, ALA204, ALA237, PHE238, ASN239, ASP255, ASN257, LEU258, SER259, GLY260, SER261, VAL262, and ALA276. The main contribution to the formation of stable supramolecular complexes of **KS1** with Tec1, Als3, and Sap3 is made by van der Waals interactions and H-bonding of the reactive groups of amino acid residues of the target proteins with **KS1** (Fig. 9).

Fluconazole is localized on the target protein site between β-sheets (s14 and s21) when interacting with Sap2 (**Supplementary Fig. 1**). The amino acid composition of the binding site is characterized by SER180, GLY181, SER182, LEU183, ILE184, ASN269, ALA270, LYS271, ILE272, LEU327, ALA328, GLN329. Stabilization of fluconazole at the protein site occurs due to a large number of intermolecular interactions of the ligand reactive groups (triazole and aromatic fragments, hydroxyl group) with the reactive groups of amino acid residues (SER182, LEU183,

Journal of
BIOLOGICAL REGULATORS
and Homeostatic Agents

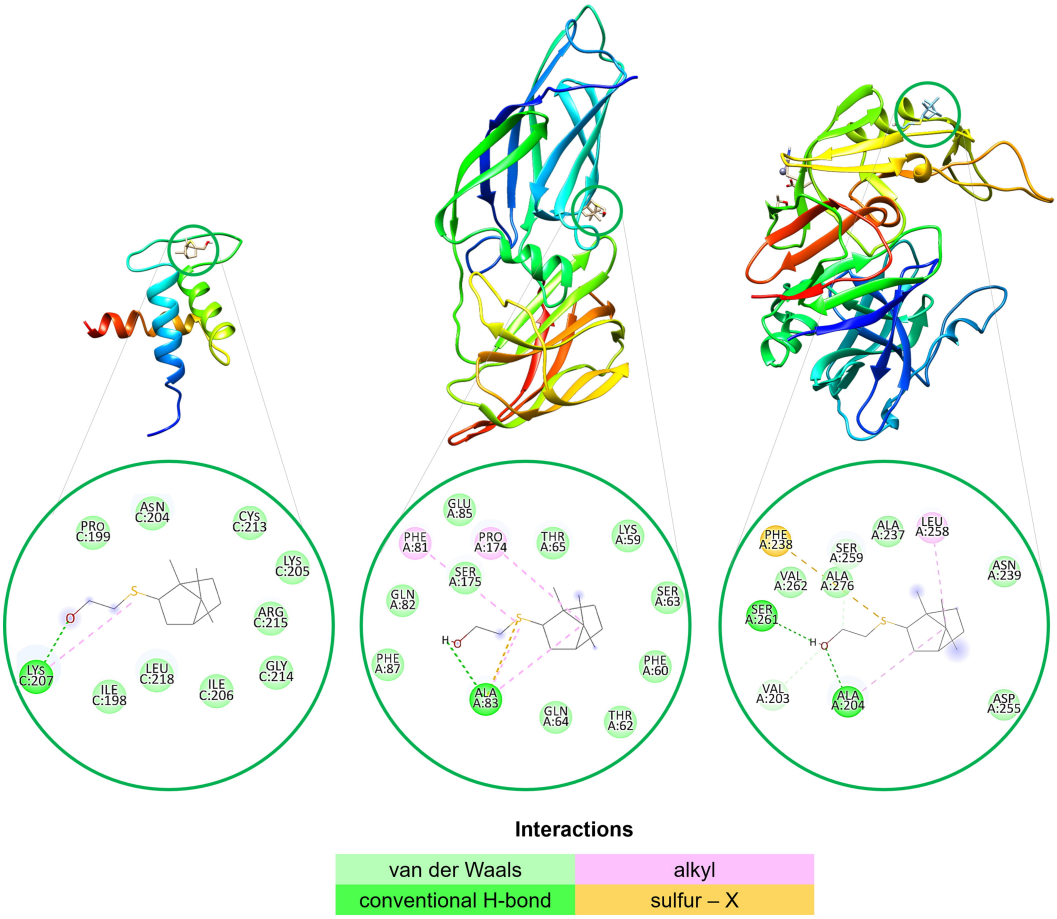

Fig. 9. Results of molecular docking for Tec1 – KS1, Als3 – KS1, and Sap3 – KS1. In the figure from left to right.

ILE184, ALA270, LYS271, SER273). Terbinafine localizes to a binding site located in the 'flap' region (a β hairpin loop) of Sap2 (**Supplementary Fig. 1**). In Sap3, fluconazole is localized in the pocket near the C-ent loops (**Supplementary Fig. 1**). The amino acid composition of binding sites includes VAL203, ALA204, ALA237, PHE238, ASN239, ASP255, LEU258, SER259, GLY260, SER261, VAL262, ALA276. Terbinafine binds to Sap3 in a similar way to Sap2 (**Supplementary Fig. 1**). In the Als3–terbinafine complex, the ligand is localized in the pocket of the N-terminal domain of Als3 [48]. The amino acid composition of the pocket is characterized by TYR21, ASN22, TYR23, THR28, SER159, ASN160, VAL161, LEU167, THR168, ASP169, SER170, TRP224, ASN225, TYR226, TRP295, ARG299.

Thus, the results of molecular docking suggest that **KS1** has the highest affinity for the transcription activator (Tec1) compared to all considered target proteins responsible for the regulation of the *C. albicans* virulence factor. This may indicate a probable inhibition of Tec1 functions by **KS1**. Along with this, it should be noted that fluconazole and terbinafine show the highest affinity for Saps, which may indicate a different mechanism of anti-candida activity compared to **KS1**.

ADMET and Drug-Likeness Properties

The electronic **Supplementary file** (see «ADMET») provides reports on ADMET and drug-likeness properties for **KS1**, fluconazole, and terbinafine. To evaluate the properties of these compounds for medicinal chemistry, we have chosen four drug similarity rules: Lipinski's rule-of-five [49], Pfizer [50], GSK [51], and Golden Triangle [52] rules. The analysis of the data obtained shows that fluconazole complies with all of the listed drug similarity rules. Terbinafine does not comply with the Pfizer Rule (LogP >3; TPSA <75) and GSK Rule (MW ≤400; LogP ≤4). According to the Pfizer Rule, compounds with a high LogP (>3) and low TPSA (Topological Polar Surface Area) (<75) are likely to be toxic. **KS1** is not subject to the Pfizer rule, and the LogP and TPSA values are 3.269 and 20.23, respectively.

Based on the value of the descriptor LogS (Log of the aqueous solubility, the range of optimal values is 0 > LogS > –4), all the studied compounds, except for terbinafine, can be classified as highly soluble in water [53]. The value of the VD descriptor (Volume Distribution, Optimal: 0.04–20 L/kg) indicates that **KS1** should have a good ability to penetrate the cell membrane.

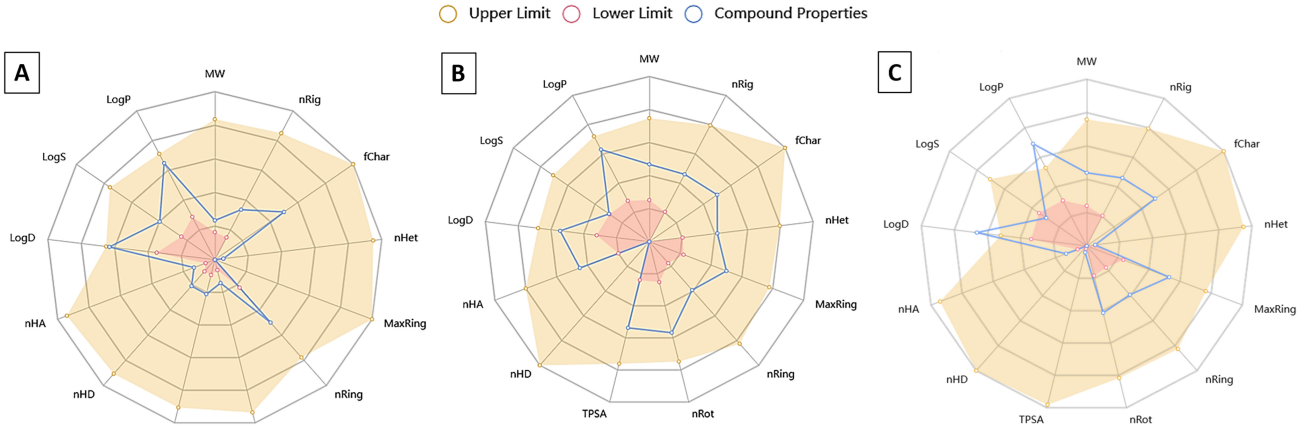

Fig. 10. Bioavailability radar depiction of compounds. KS1 (A), fluconazole (B), and terbinafine (C) (MW, molecular weight; nRig, number of rigid bonds; fChar, formal charge; nHet, number of heteroatoms; MaxRing, number of atoms in the biggest ring; nRing, number of rings; nRot, number of rotatable bonds; TPSA, topological polar surface area; nHD, number of hydrogen bond donors; nHA, number of hydrogen bond acceptors; LogP, log of the octanol/water partition coefficient; LogD, log of the octanol/water (at physiological pH 7.4) partition coefficient; LogS, log of the aqueous solubility).

When discussing the metabolism of the compounds under consideration, attention should be paid to their activity towards an important metabolic enzyme, cytochrome P450, namely, its main isoforms: CYP1A2, CYP2C19, CYP2C9, CYP2D6, and CYP3A4 [54]. It was found that fluconazole looks like an inhibitor of the human cytochrome P450 system, especially the isoenzymes CYP1A2 and CYP2C19 (to a lesser extent CYP3A4 and CYP2C9). In turn, terbinafine is able to inhibit isoenzymes CYP2C19, CYP2D6 (to a lesser extent CYP1A2, CYP3A4). Thus, theoretically, fluconazole and terbinafine are able to reduce the metabolism of the cell. Compared to fluconazole and terbinafine, **KS1** has no ability to inhibit these enzymes, which indicates the safety of their pharmacokinetics. An evaluation of the total clearance showed that all the studied compounds have average values of the body cleansing coefficient (5–15 mL/min per kg). The toxicity evaluation (AMES Toxicity) of the studied compounds showed that, compared to terbinafine, **KS1** carcinogenicity is uncharacteristic. In addition, all of the considered compounds are not hERG inhibitors.

Fig. 10 presents the bioavailability of drug-likeness properties for **KS1** and reference compounds. The blue line characterizing the properties of a compound must lie between the lower limit and the upper limit in order to classify it as drug-like. It can be seen from the bioavailability radar that all compounds under consideration are in the optimal range of drug-likeness properties, with the exception of terbinafine, which has a deviation in LogP, LogS, and LogD.

Thus, the analysis of ADMET and drug-likeness properties for **KS1** showed that it belongs to drug-like compounds. And, unlike reference compounds, they do not inhibit isoforms of cytochrome P450 and do not show mutagenicity and carcinogenicity.

Discussion

To date, the wide spread of multidrug-resistant opportunistic yeast *C. albicans* occurs all over the world, and the efficiency of candidiasis treatment decreases [1–4], thus challenging the development of either new antifungals or increasing the efficiency of existing ones. Among various options, the use of natural and synthetic terpenes as antifungals or enhancers of conventional drugs has been offered in many works [14–21].

In this study, we demonstrated the potential of the synthetic isobornane sulfide named **KS1** as an antifungal agent and enhancer of conventional antifungals. While solely **KS1** exhibits moderate antifungal activity as compared to fluconazole and terbinafine, it represses the germ tubes formation up to 2-fold compared to untreated cells, while sub-inhibitory concentrations of both reference antimycotics induce the morphological transition of *C. albicans* cells to pseudomycelium form, one of the virulence factors of these yeast [1,22]. This fact characterizes **KS1** as a promising tool for decreasing the invasion of yeasts, consequently facilitating the natural elimination of infectious agents from the host organism without the development of resistance [10]. Importantly, **KS1** leads neither to resistance formation nor an increase in the expression of the *CDR1* and *MDR1* efflux genes, making the compound save from resistance development and its spread. A similar *in vitro* repression of *C. albicans* adhesion properties and morphological transition were reported for another terpene, Limonene, via apparent repression of Plb1 and Tec1 proteins [21]. The molecular docking of **KS1** with a number of proteins responsible for invasion demonstrated high affinity to secreted aspartic proteases Sap3 and Sap5, as well as with Plb1 and Tec1. These data fit with earlier reported data for limonene and allow assuming apparently similar-

Journal of
BIOLOGICAL REGULATORS
and Homeostatic Agents

ity in the mechanisms of action of various terpenes. Furthermore, Borelli *et al*. [46] have demonstrated that Sap1-3 and Sap5 share a highly conserved secondary structure and thus represent an universal target in *Candida* isolates. However, the structure of Sap5 differs from Sap1-3 in terms of its overall electrostatic charge as well as the structural conformation of the active site. In our opinion, these differences between Saps should be considered when developing drugs with selectivity for inhibiting a specific protein target. Furthermore, since *C. albicans* produces many virulence factors including four hypha-associated proteins (HWP1, ECE1, HYR1 and ALS3), lipases, phospholipases and adhesins [22], the **KS1** treatment theoretically can lead to pleotropic effect via either direct interaction with proteins or repression of genes expression. Thus, a detailed evaluation of how compound represses the growth and pseudomycelium formation by the yeast is required.

Importantly, **KS1** exhibited a synergistic effect with both fluconazole and terbinafine on resistant clinical isolates, reducing the MIC of antifungals 10–50 times. Interestingly, a clear synergy was observed on resistant strains, while the MIC on sensitive strains was reduced only 2–4-fold. The mechanism of how terpenes increase the efficiency of antimicrobials remains discussible, despite various works demonstrating this effect [16–19,55,56]. Since terpenes have membranotropic properties, it has been proposed that these compounds, alone or fused with other pharmacophores, could damage the membrane of the cell [19,57,58]. Therefore, the conjugate of **KS1** with BODIPY was used to evaluate the penetration of the compound into the cell as well as into the biofilm-embedded cells. Both pure BODIPY **2** and conjugate **3** were able to get inside the cells and stain the nucleus, thus limiting the clear decision about the ability of **KS1** to penetrate the cell. Nevertheless, BODIPY **2** penetrated poorly into the “old” cells of the *C. albicans*, while conjugate **3** was able to penetrate all cells. This fact suggests that **KS1** penetrates through the cell membrane and thus apparently facilitating the penetration of the fluconazole and terbinafine via changes of the membrane properties. This could also explain the marked increase the susceptibility of resistant strains, which apparently have low permeability of the membrane for drugs. Finally, while the *MDR1* and *CDR1* were reported to be induced in response to oxidative stress [37,59], it could be speculated that **KS1** rather changes the permeability of membranes of cell and organelles than leads to their dramatic damage. By contrast, the CLSM-analysis revealed lower speed on **KS1**-BODIPY 3 penetration in the biofilm of a fluconazole-resistant strain since the intensity of fluorescence was considerably lower. This could be because of different structure of either the cell wall of sensitive and resistant cells or the biofilm matrix structure. Nevertheless, the mechanisms by which **KS1** affects the yeast remain and require further investigation.

Conclusions

Taken together, our data allow for the suggestion of **KS1** as a tool to increase the susceptibility of tolerant *C. albicans* isolates to antifungals and block the virulence of the yeasts. Our data clearly show that **KS1** can penetrate both planktonic and biofilm-embedded cells, and in combination with conventional antifungals, it represents an antifungal treatment approach. With no mutagenicity and low toxicity, it appears as a promising therapeutic agent to increase the efficiency of the treatment of candidiasis mediated by resistant strains. Nevertheless, the mechanisms of how **KS1** and other terpenes affect the yeast remain still unclear and thus limit their application yet. The unraveling of molecular targets for terpenes would open the door to the construction of bi-pharmacophore drugs with high permeability into fungal cells, thus reducing side effects for the host and decreasing the risk of resistance development.

Availability of Data and Materials

Data are available by request.

Author Contributions

SAL, LEN, AAR and ARK designed the research study. SAL, AAK, PSB, MOS, OVO, EYT, IRG, RSP, SVP, ESI and AGI performed the research. EVA, GBG, MBB, SAR provided help and advice on synthetic procedures. SAL, AAK, LEN, AAR and ARK analyzed the data. SAL, AAK, IRG, AAR, LEN and ARK wrote the manuscript. All authors contributed to editorial changes in the manuscript. All authors read and approved the final manuscript. All authors have participated sufficiently in the work and agreed to be accountable for all aspects of the work.

Ethics Approval and Consent to Participate

Not applicable.

Acknowledgment

This work was supported by the Kazan Federal University Strategic Academic Leadership program (PRIORITY-2030).

Funding

The study of biological activity was conducted with the financial support of the Russian Science Foundation (grant N 20-64-47014).

Conflict of Interest

The authors declare no conflict of interest.

Supplementary Material

Supplementary material associated with this article can be found, in the online version, at https://doi.org/10.23812/j.biol.regul.homeost.agents.20243805.291.

References

[1] Naglik J, Albrecht A, Bader O, Hube B. Candida albicans proteinases and host/pathogen interactions. Cellular Microbiology. 2004; 6: 915–926.

[2] Bongomin F, Gago S, Oladele RO, Denning DW. Global and Multi-National Prevalence of Fungal Diseases-Estimate Precision. Journal of Fungi (Basel, Switzerland). 2017; 3: 57.

[3] Achkar JM, Fries BC. Candida infections of the genitourinary tract. Clinical Microbiology Reviews. 2010; 23: 253–273.

[4] Kumari V, Banerjee T, Kumar P, Pandey S, Tilak R. Emergence of non-albicans Candida among candidal vulvovaginitis cases and study of their potential virulence factors, from a tertiary care center, North India. Indian Journal of Pathology & Microbiology. 2013; 56: 144–147.

[5] Singh DK, Tóth R, Gácser A. Mechanisms of Pathogenic *Candida* Species to Evade the Host Complement Attack. Frontiers in Cellular and Infection Microbiology. 2020; 10: 94.

[6] Xiao Z, Wang Q, Zhu F, An Y. Epidemiology, species distribution, antifungal susceptibility and mortality risk factors of candidemia among critically ill patients: a retrospective study from 2011 to 2017 in a teaching hospital in China. Antimicrobial Resistance and Infection Control. 2019; 8: 89.

[7] Gulshan K, Moye-Rowley WS. Multidrug resistance in fungi. Eukaryotic Cell. 2007; 6: 1933–1942.

[8] de Oliveira Santos GC, Vasconcelos CC, Lopes AJO, de Sousa Cartágenes MDS, Filho AKDB, do Nascimento FRF, *et al*. *Candida* Infections and Therapeutic Strategies: Mechanisms of Action for Traditional and Alternative Agents. Frontiers in Microbiology. 2018; 9: 1351.

[9] Shahid Z, Sobel JD. Reduced fluconazole susceptibility of Candida albicans isolates in women with recurrent vulvovaginal candidiasis: effects of long-term fluconazole therapy. Diagnostic Microbiology and Infectious Disease. 2009; 64: 354–356.

[10] Fernandes L, Ribeiro R, Henriques M, Rodrigues ME. Candida auris, a singular emergent pathogenic yeast: its resistance and new therapeutic alternatives. European Journal of Clinical Microbiology & Infectious Diseases: Official Publication of the European Society of Clinical Microbiology. 2022; 41: 1371–1385.

[11] Parker RA, Gabriel KT, Graham KD, Butts BK, Cornelison CT. Antifungal Activity of Select Essential Oils against *Candida auris* and Their Interactions with Antifungal Drugs. Pathogens (Basel, Switzerland). 2022; 11: 821.

[12] Tran HNH, Graham L, Adukwu EC. In vitro antifungal activity of Cinnamomum zeylanicum bark and leaf essential oils against Candida albicans and Candida auris. Applied Microbiology and Biotechnology. 2020; 104: 8911–8924.

[13] Wenji KY, Rukmi I, Suprihadi A. In vitro Antifungal Activity of Methanolic and Chloroform Mint Leaves (Mentha piperita L.) Extracts Against Candida albicans. Journal of Physics: Conference Series. 2019; 1217: 012136.

[14] Szczepanski S, Lipski A. Essential oils show specific inhibiting effects on bacterial biofilm formation. Food Control. 2014; 36; 224–229.

[15] Guimarães AC, Meireles LM, Lemos MF, Guimarães MCC, Endringer DC, Fronza M, *et al*. Antibacterial Activity of Terpenes and Terpenoids Present in Essential Oils. Molecules (Basel, Switzerland). 2019; 24: 2471.

[16] Cavalcanti BB, Neto HD, da Silva-Rocha WP, de Oliveira Lima E, Barbosa Filho JM, de Castro RD, *et al*. Inhibitory Effect of (–)-myrtenol alone and in combination with antifungal agents on Candida spp. Research, Society and Development. 2021; 10: e35101522434–e35101522434.

[17] Maione A, La Pietra A, de Alteriis E, Mileo A, De Falco M, Guida M, *et al*. Effect of Myrtenol and Its Synergistic Interactions with Antimicrobial Drugs in the Inhibition of Single and Mixed Biofilms of *Candida auris* and *Klebsiella pneumoniae*. Microorganisms. 2022; 10: 1773.

[18] Sulaiman R, Trizna E, Kolesnikova A, Khabibrakhmanova A, Kurbangalieva A, Bogachev M, *et al*. Antimicrobial and Biofilm-Preventing Activity of l-Borneol Possessing 2(5H)-Furanone Derivative F131 against S. aureus—C. albicans Mixed Cultures. Pathogens (Basel, Switzerland). 2022; 12: 26.

[19] Mahmoud RY, Trizna EY, Sulaiman RK, Pavelyev RS, Gilfanov IR, Lisovskaya SA, *et al*. Increasing the Efficacy of Treatment of *Staphylococcus aureus-Candida albicans* Mixed Infections with Myrtenol. Antibiotics (Basel, Switzerland). 2022; 11: 1743.

[20] Uppar V, Chandrashekharappa S, Shivamallu C, Shushma P, Kollur SP, Ortega-Castro J, *et al*. Investigation of Antifungal Properties of Synthetic Dimethyl-4-Bromo-1-(Substituted Benzoyl) Pyrrolo[1,2-a] Quinoline-2,3-Dicarboxylates Analogues: Molecular Docking Studies and Conceptual DFT-Based Chemical Reactivity Descriptors and Pharmacokinetics Evaluation. Molecules. 2021; 26: 2722.

[21] Ahmedi S, Pant P, Raj N, Manzoor N. Limonene inhibits virulence associated traits in Candida albicans: In-vitro and in-silico studies. Phytomedicine Plus. 2022; 2: 100285.

[22] Mayer FL, Wilson D, Hube B. Candida albicans pathogenicity mechanisms. Virulence. 2013; 4: 119–128.

[23] Wu H, Downs D, Ghosh K, Ghosh AK, Staib P, Monod M, *et al*. Candida albicans secreted aspartic proteases 4-6 induce apoptosis of epithelial cells by a novel Trojan horse mechanism. FASEB Journal: Official Publication of the Federation of American Societies for Experimental Biology. 2013; 27: 2132–2144.

[24] Lodochnikova OA, Islamov DR, Gerasimova DP, Zakharychev DV, Saifina AF, Pestova SV, *et al*. Isobornanyl sulfoxides and isobornanyl sulfone: Physicochemical characteristics and the features of crystal structure. Journal of Molecular Structure. 2021; 1239: 130491.

[25] Guseva G, Antina E, Berezin M, Lisovskaya S, Pavelyev R, Kayumov A, *et al*. Spectroscopic and In Vitro Investigations of Boron(III) Complex with *Meso*-4-Methoxycarbonylpropylsubstituted Dipyrromethene for Fluorescence Bioimaging Applications. Molecules (Basel, Switzerland). 2020; 25: 4541.

[26] Guseva GB, Antina EV, Berezin MB, Pavelyev RS, Kayumov AR, Ostolopovskaya OV, *et al*. Design, Spectral Characteristics, and Possibilities for Practical Application of BODIPY FL-Labeled Monoterpenoid. ACS Applied Bio Materials. 2021; 4: 6227–6235.

[27] Guseva GB, Antina EV, Berezin MB, Smirnova AS, Pavelyev RS, Gilfanov IR, *et al*. Design, Spectral Characteristics, Photostability, and Possibilities for Practical Application of BODIPY FL-Labeled Thioterpenoid. Bioengineering (Basel, Switzerland). 2022; 9: 210.

[28] Xiong G, Wu Z, Yi J, Fu L, Yang Z, Hsieh C, *et al*. ADMETlab 2.0: an integrated online platform for accurate and comprehensive predictions of ADMET properties. Nucleic Acids Research. 2021; 49: W5–W14.

[29] Morris GM, Huey R, Lindstrom W, Sanner MF, Belew RK, Goodsell DS, *et al*. AutoDock4 and AutoDockTools4: Automated docking with selective receptor flexibility. Journal of Computational Chemistry. 2009; 30: 2785–2791.

[30] Bannwarth C, Grimme S. A simplified time-dependent density

functional theory approach for electronic ultraviolet and circular dichroism spectra of very large molecules. Computational and Theoretical Chemistry. 2014; 1040–1041: 45–53.

[31] Dunning T. Gaussian basis sets for use in correlated molecular calculations. I. The atoms boron through neon and hydrogen. The Journal of Chemical Physics. 1989; 90: 1007.

[32] Solis FJ, Wets RJ-B. Minimization by Random Search Techniques. Mathematics of Operations Research. 1981; 6: 19–30.

[33] Raush ER, Vybornova IV, Shagdileeva EV, Vasilyeva NV, Bogomolova TS, Khostelidi SN, *et al*. Susceptibility testing of invasive candidosis pathogens to Fluconazole and Voriconazole by international standards. Problems in Medical Mycology. 2013; 15: 60–63. (In Russian)

[34] Garipov MR, Sabirova AE, Pavelyev RS, Shtyrlin NV, Lisovskaya SA, Bondar OV, *et al*. Targeting pathogenic fungi, bacteria and fungal-bacterial biofilms by newly synthesized quaternary ammonium derivative of pyridoxine and terbinafine with dual action profile. Bioorganic Chemistry. 2020; 104: 104306.

[35] den Hollander JG, Mouton JW, Verbrugh HA. Use of pharmacodynamic parameters to predict efficacy of combination therapy by using fractional inhibitory concentration kinetics. Antimicrobial Agents and Chemotherapy. 1998; 42: 744–748.

[36] Pollard JE, Snarr J, Chaudhary V, Jennings JD, Shaw H, Christiansen B, *et al*. In vitro evaluation of the potential for resistance development to ceragenin CSA-13. The Journal of Antimicrobial Chemotherapy. 2012; 67: 2665–2672.

[37] Watamoto T, Samaranayake LP, Egusa H, Yatani H, Seneviratne CJ. Transcriptional regulation of drug-resistance genes in Candida albicans biofilms in response to antifungals. Journal of Medical Microbiology. 2011; 60: 1241–1247.

[38] Jia W, Zhang H, Li C, Li G, Liu X, Wei J. The calcineruin inhibitor cyclosporine a synergistically enhances the susceptibility of Candida albicans biofilms to fluconazole by multiple mechanisms. BMC Microbiology. 2016; 16: 113.

[39] Zheng L, Duan Z, Tang D, He Y, Chen X, Chen Q, *et al*. GP IIb/IIIa-Mediated Platelet Activation and Its Modulation of the Immune Response of Monocytes Against *Candida albicans*. Frontiers in Cellular and Infection Microbiology. 2021; 11: 783085.

[40] Bogachev MI, Volkov VY, Markelov OA, Trizna EY, Baydamshina DR, Melnikov V, *et al*. Fast and simple tool for the quantification of biofilm-embedded cells sub-populations from fluorescent microscopic images. PLoS ONE. 2018; 13: e0193267.

[41] Bogachev MI, Volkov VY, Kolaev G, Chernova L, Vishnyakov I, Kayumov A. Selection and quantification of objects in microscopic images: from multi-criteria to multi-threshold analysis. BioNanoScience. 2019; 9: 59–65.

[42] Nikitina L, Lisovskaya S, Startseva V, Pavelyev R, Gilfanov I, Fedyunina I, *et al*. Development of Novel Effective Agents Against Candida albicans Biofilms. BioNanoScience. 2019; 9: 539–544.

[43] McCann J, Ames BN. A simple method for detecting environmental carcinogens as mutagens. Annals of the New York Academy of Sciences. 1976; 271: 5–13.

[44] Mukhamedyarov MA, Rizvanov AA, Yakupov EZ, Zefirov AL, Kiyasov AP, Reis HJ, *et al*. Transcriptional Analysis of Blood Lymphocytes and Skin Fibroblasts, Keratinocytes, and Endothelial Cells as a Potential Biomarker for Alzheimer's Disease. Journal of Alzheimer's Disease. 2016; 54: 1373–1383.

[45] Borelli C, Ruge E, Schaller M, Monod M, Korting HC, Huber R, *et al*. The crystal structure of the secreted aspartic proteinase 3 from Candida albicans and its complex with pepstatin A. Proteins. 2007; 68: 738–748.

[46] Borelli C, Ruge E, Lee JH, Schaller M, Vogelsang A, Monod M, *et al*. X-ray structures of Sap1 and Sap5: structural comparison of the secreted aspartic proteinases from Candida albicans. Proteins. 2008; 72: 1308–1319.

[47] Cutfield SM, Dodson EJ, Anderson BF, Moody PC, Marshall CJ, Sullivan PA, *et al*. The crystal structure of a major secreted aspartic proteinase from Candida albicans in complexes with two inhibitors. Structure. 1995; 3: 1261–1271.

[48] Hoyer LL, Cota E. Candida albicans Agglutinin-Like Sequence (Als) Family Vignettes: A Review of Als Protein Structure and Function. Frontiers in Microbiology. 2016; 7: 280.

[49] Lipinski CA, Lombardo F, Dominy BW, Feeney PJ. Experimental and computational approaches to estimate solubility and permeability in drug discovery and development settings. Advanced Drug Delivery Reviews. 2001; 46: 3–26.

[50] Hughes JD, Blagg J, Price DA, Bailey S, Decrescenzo GA, Devraj RV, *et al*. Physiochemical drug properties associated with in vivo toxicological outcomes. Bioorganic & Medicinal Chemistry Letters. 2008; 18: 4872–4875.

[51] Gleeson MP. Generation of a set of simple, interpretable ADMET rules of thumb. Journal of Medicinal Chemistry. 2008; 51: 817–834.

[52] Johnson TW, Dress KR, Edwards M. Using the Golden Triangle to optimize clearance and oral absorption. Bioorganic & Medicinal Chemistry Letters. 2009; 19: 5560–5564.

[53] Wang Y, Xing J, Xu Y, Zhou N, Peng J, Xiong Z, *et al*. In silico ADME/T modelling for rational drug design. Quarterly Reviews of Biophysics. 2015; 48: 488–515.

[54] Farsang C, Fischer J. Optimizing Antihypertensive Therapy by Angiotensin Receptor Blockers. Analogue-Based Drug Discovery. 2006; 157–168.

[55] Kifer D, Mužinić V, Klarić MŠ. Antimicrobial potency of single and combined mupirocin and monoterpenes, thymol, menthol and 1,8-cineole against Staphylococcus aureus planktonic and biofilm growth. The Journal of Antibiotics. 2016; 69: 689–696.

[56] Zacchino SA, Butassi E, Cordisco E, Svetaz LA. Hybrid combinations containing natural products and antimicrobial drugs that interfere with bacterial and fungal biofilms. Phytomedicine: International Journal of Phytotherapy and Phytopharmacology. 2017; 37: 14–26.

[57] Sharafutdinov IS, Pavlova AS, Akhatova FS, Khabibrakhmanova AM, Rozhina EV, Romanova YJ, *et al*. Unraveling the Molecular Mechanism of Selective Antimicrobial Activity of 2(5*H*)-Furanone Derivative against *Staphylococcus aureus*. International Journal of Molecular Sciences. 2019; 20: 694.

[58] Sharafutdinov IS, Ozhegov GD, Sabirova AE, Novikova VV, Lisovskaya SA, Khabibrakhmanova AM, *et al*. Increasing Susceptibility of Drug-Resistant *Candida albicans* to Fluconazole and Terbinafine by 2(5*H*)-Furanone Derivative. Molecules. 2020; 25: 642.

[59] Larsen B, Anderson S, Brockman A, Essmann M, Schmidt M. Key physiological differences in Candida albicans *CDR1* induction by steroid hormones and antifungal drugs. Yeast. 2006; 23: 795–802.